ANISOTROPIC EXCITATION TRANSFER TO ACCEPTORS RANDOMLY DISTRIBUTED ON SURFACES

H. KELLERER AND A. BLUMEN
Lehrstuhl für Theoretische Chemie, Technische Universität München, D-8046 Garching, Federal Republic of Germany

ABSTRACT We presented exact expressions for the ensemble averaged decay of the excitation of a donor molecule due to the energy transfer via anisotropic dipolar interactions to acceptors distributed randomly on a surface. The disorder extended both over the positions of the acceptors and over the orientations of their transition dipoles with respect to that of the donor molecule. Several cases were considered explicitly (*a*) random orientations of the acceptors in space, with the donor being (*a1*) perpendicular to the plane, (*a2*) in the plane, (*a3*) randomly oriented in space; (*b*) random orientations of both donor and acceptors in the plane; (*c*) parallel orientations of donor and acceptors (no orientational disorder). For all these cases we evaluated the analytic, Förster-like expressions, valid for long times and low acceptor densities, and obtained their domains of validity by comparison with the exact, numerically calculated decay laws.

INTRODUCTION

Fluorescence energy transfer is a valuable technique in determining microscopic parameters, such as intermolecular distances and interactions in biological systems. In a recent series of papers in this journal (1–5) much attention has been paid to energy transfer mechanisms in two-dimensional molecular assemblies. The applications of the techniques for membranes and phospholipid vesicles range from studies on membrane fusion and on antibody-receptor clustering to the determination of lipid-protein interactions and of bilayer spacings. On the other hand, theoretical treatments of energy transfer problems in three dimensions have a long history, and the modern treatments have been deeply influenced by the work of Förster (6).

A basic problem one faces when treating the energy transfer to randomly distributed acceptors is the proper ensemble averaging; the problem arises because the experimentally measurable decay of the donor excitation stems from many excited donor molecules, each surrounded by its own configuration of acceptor molecules. In a very elegant way, Förster has obtained an approximate ensemble-averaged formula through a limiting process; his final expression has the virtue of being very simple, but it holds only for low acceptor concentrations and for times long compared with the most rapid transfer possible; also, the formula neglects the influence of the intermolecular separations (7, 8). One can, of course, introduce a-posteriori the effect of a minimal intermolecular distance into Förster's expressions (either analytically [1] or via Monte-Carlo calculations of the true average [5]), but the procedure is cumbersome.

Interestingly, however, one is not bound to use Förster's procedure of averaging to obtain his decay laws. As summarized by Blumen (8) this is due to the fact that the ensemble-averaged decay law can be expressed exactly, in closed form. The expression holds for arbitrary concentrations of acceptors and donor-acceptor interactions and for all times; implicitly included in this formula is the underlying molecular structure and thus also the distance of nearest approach. From this exact expression, whole series of approximate formulas (including Förster's) follow (8).

Here we treat the energy transfer from a donor to acceptors via anisotropic dipolar interactions. Thus we take into account both the randomness in the positions and also in the orientations of the acceptor molecules and present both exact and approximate decay laws. This will exemplify the flexibility of our approach. We concentrate on two-dimensional assemblies (for three-dimensional systems, see reference 9) because these are of much biophysical interest. Also the question of the proper averaging of the anisotropic part of the dipolar interaction is significant. Evidently, the orientation of the molecular dipoles is of importance in depolarization experiments used to determine molecular separations (2); thus, in the use of energy transfer as a "spectroscopic ruler" (for a review see Stryer, reference 10), one has to take orientational factors into account. As pointed out by Knox (11), the information submerged by the prior averaging over the angular distributions can be very significant. As we will show, in special arrangements the effect of anisotropic interactions is very pronounced and may be used in gaining insight in the microscopic structure. More generally, the anisotropies lead to changes even in the coefficients of the Förster-type decays. Corresponding factors for three-dimensional cases have been previously obtained (9, 12); to our best knowledge, however, we are the first to determine analytically the corresponding factors for two-dimensional geometries.

In the Theory section we derive the basic theoretical expressions using the exact averaging procedures; there we also specialize our expressions to the two-dimensional geometry by considering several orientational arrangements; as will become evident, this problem is richer than its three-dimensional counterpart (see reference 9). In the Results section we present numerical results for the decay laws and compare the exact decays with the Förster-like forms, determining the domains of validity of the latter. The paper closes with a summary of conclusions, where we also make connection to the previous works.

THEORY

Here we present the ensemble-averaged decay of the excitation of a donor, surrounded by randomly distributed acceptors. We center mainly on the energy transfer process and note from the start that generally the intramolecular (radiative and radiationless) decay channels are transfer independent. Thus, denoting the radiative decay rate by τ_R^{-1} and the intramolecular decay rate by τ_N^{-1}, the effect of these factors is readily incorporated in the results that follow by multiplying by $\exp[-t\,(\tau_R^{-1} + \tau_N^{-1})]$, or setting $\tau_D^{-1} \equiv \tau_R^{-1} + \tau_N^{-1}$ by $\exp[-t/\tau_D]$. It suffices then to consider the energy transfer mechanism separately, and to include, whenever necessary, this multiplicative factor.

The rate of energy transfer from the donor to an acceptor molecule, $w_\alpha(\mathbf{R})$, depends on the mutual distance $\mathbf{R}$ and, in general, on additional factors, which we denote by α. For dipolar interactions, which we will consider in the following (other types of interactions are discussed in reference 9), these factors are the orientations of the transition dipoles $\mathbf{e}_D$ and $\mathbf{e}_A$ of the donor and of the acceptor, and the orientation $\mathbf{e}_R = \mathbf{R}/R$ of the vector $\mathbf{R}$. To a good approximation, one has

$$w_\alpha(\mathbf{R}) = \frac{\kappa^2}{\tau}\left(\frac{d}{R}\right)^6 \tag{1}$$

with

$$\kappa = \mathbf{e}_D \cdot \mathbf{e}_A - 3(\mathbf{e}_D \cdot \mathbf{e}_R)(\mathbf{e}_A \cdot \mathbf{e}_R). \tag{2}$$

In Eq. 1, d is the distance of nearest possible approach between donor and acceptor, and, as in former works (7–9), we prefer to scale $w_\alpha(\mathbf{R})$ with respect to d; τ^{-1} is then the transfer rate of a nearest-neighbor donor-acceptor pair whose transition dipoles are oriented parallel to each other and perpendicular to $\mathbf{e}_R$. This notation dispenses with a comparison to the radiative lifetime, τ_R; the more usual notation, based on reference 6, obtains by introducing the Förster radius R_0, so that $3\,R_0^6/(2\,\tau_R) = d^6/\tau$.

We hasten to add that Eqs. 1 and 2 are only approximations; realistic transfer rates may have a considerably more complex structure. Also, a quantum mechanical derivation for Eq. 1 presupposes that, compared with the energy of the heat bath, the two molecules are very weakly coupled (13). Assuming Eq. 1 to hold also at short distances implies that the vibrational relaxation is very fast on the time scale of the energy transfer. Fortunately, in most biological applications these conditions are satisfied (11, 14, 15) so that we will use Eqs. 1 and 2 in the following. For dipolar interactions (but not for higher multipolar or for exchange interactions), the parameter τ (or R_0, equivalently) may be obtained from the line shapes of the absorption and emission spectra (13, 14).

The transition rate $w_\alpha(\mathbf{R})$, Eq. 1, depends both on the vector $\mathbf{R}$ and on the orientations of the transition dipoles. If the rotational motion of the molecules is very fast compared with the energy transfer, one can simplify the model by first averaging $w_\alpha(\mathbf{R})$ with respect to the angular dependence

$$w(R) \equiv \langle w_\alpha(\mathbf{R})\rangle = \frac{\langle\kappa^2\rangle}{\tau}\left(\frac{d}{R}\right)^6. \tag{3}$$

Such a simplification is not justified, however, when on the time scale of the transfer, the molecular orientations do not change; here one has to use the unaveraged $w_\alpha(\mathbf{R})$ form.

Consider now both donor and acceptors embedded in a solid or in a membrane. We place the donor at the origin and distribute the acceptors on a set of sites $\mathbf{R}_j$. Each site has the probability p of being occupied, so that the distribution of acceptors will be random. Focusing now on a particular acceptor configuration $\mathbf{K}$ in which the sites $\mathbf{R}_j$ are occupied, $\mathbf{K} = \{j\}$, we obtain for the decay law of the donor excitation

$$\Phi(\mathbf{K}; t) = \exp\left[-t\sum_{j\in\mathbf{K}} w_{\alpha j}(\mathbf{R}_j)\right] = \prod_{j\in\mathbf{K}} \exp[-tw_{\alpha j}(\mathbf{R}_j)]. \tag{4}$$

Note that the decay given by Eq. 4 is exponential.

The quantity of interest experimentally is not $\Phi(\mathbf{K}; t)$, the decay due to a particular acceptor configuration $\mathbf{K}$, but the ensemble average of $\Phi(\mathbf{K}; t)$ over all possible acceptor configurations. Fortunately, the average of Eq. 4 over the spatial coordinates, $\mathbf{R}_j$, as well as over the angular functions, α_j, can be performed exactly (7–9). To exemplify the procedure, we focus first on the spatial averaging and perform it for the angularly preaveraged interaction $w(R)$. From Eq. 4

$$\Phi(\mathbf{K}; t) = \prod_{j\in\mathbf{K}} \exp\,[-tw(\mathbf{R}_j)] = \prod_i \exp\,[-t\eta_i w(\mathbf{R}_i)], \tag{5}$$

with $\eta_i = 1$ if $i \in \mathbf{K}$ and $\eta_i = 0$ otherwise. The spatial average is now

$$\Phi(t) = \langle\Phi(\mathbf{K}; t)\rangle_{\{\eta_i\}} = \prod_i \langle\exp\,[-t\eta_i w(\mathbf{R}_i)]\rangle_{\eta_i}$$

$$= \prod_i \{1 - p + p\exp\,[-tw(\mathbf{R}_i)]\}. \tag{6}$$

Note that Eq. 6 is exact, and that the product extends over all sites i. Eq. 6 has been derived in different ways by several authors; see works cited in reference 8.

Turning now to the general case, we have to use a continuous probability density $g(\alpha)$; then $pg(\alpha)d\alpha$ is the joint probability that a site is occupied and that the orientations result in a value α_0 with $\alpha < \alpha_0 < \alpha + d\alpha$. As a straightforward extension of Eq. 6 one has

$$\Phi(t) = \prod_i \{1 - p + pE(t; \mathbf{R}_i)\} \tag{7}$$

with

$$E(t; \mathbf{R}) = \int d\alpha\, g(\alpha)\exp[-tw_\alpha(\mathbf{R})]. \tag{8}$$

A different derivation of Eq. 7 was presented in reference 9.

The two exact expressions, Eqs. 6 and 7, will be used in the following to determine the decay laws for several two-dimensional models. We proceed by first making connection to Förster-type expressions.

We start with the classical case, Eq. 6. Taking logarithms on both sides and expanding in powers of p, $p < 1$, we have

$$\ln\Phi(t) = \sum_i \ln\{1 - p[1 - \exp\,(-tw(\mathbf{R}_i)]\}$$

$$= -\sum_{k=1}^{\infty}(p^k/k)\sum_i \{1 - \exp\,[-tw\,(\mathbf{R}_i)]\}^k, \tag{9}$$

which for small concentrations of acceptors ($p \ll 1$) may be approximated by

$$\ln \Phi(t) \approx -p \sum_i \{1 - \exp[-tw(\mathbf{R}_i)]\}. \quad (10)$$

Note that we can take care of all geometrical constraints by proper restrictions on the sum over i. The sum can also be approximated by an integral over the spatial region under consideration. For instance, for an infinite plane

$$\ln \Phi(t) \approx -2\pi p\rho \int_0^\infty dRR\{1 - \exp[-tw(R)]\}, \quad (11)$$

where ρ is the density of sites in the plane, and thus $p\rho$ is the planar concentration of acceptors. Introducing now the interaction, Eq. 3, and performing the integration in Eq. 11, we obtained

$$\Phi(t) = \exp\{-Cp\rho d^2(t/\tau)^{1/3}\}, \quad (12)$$

with C being a constant, $C = \pi\,\Gamma(\frac{2}{3})\,\langle\kappa^2\rangle^{1/3}$. Here $\Gamma(x)$ denotes the Euler gamma function, Eqs. 6.1.1 of Abramovitz and Stegun (16). With $\langle\kappa^2\rangle = \frac{2}{3}$, and thus $C = 3.71629$, Eq. 12 is identical to Eq. 13 of Wolber and Hudson (1), obtained using the Förster-limiting process, and also to Eq. 3.15 of Blumen and Manz (7). The interesting aspect of Eq. 12 is the fractional exponent of the time, which here equals $\frac{1}{3}$. Such fractional exponents appear readily under averaging conditions of the type that we consider. As discussed in reference 7, generally, the exponent equals Δ/s, where Δ is the dimension (here $\Delta = 2$) and s is the inverse power of R in $w(R)$, here $s = 6$. We note that extensions of Eq. 12 are now readily obtainable. First, by remarking that there exists a minimal distance of nearest approach, and thus starting the integration in Eq. 11 at a finite distance instead of at 0 (see references 1 and 7); second by going to higher concentrations and taking additional powers of p from Eq. 9 into account. We will not pursue these approaches here; to determine the domain of validity of equations like Eq. 12 we compare directly Eqs. 6 and 7, which we evaluated numerically, with the exact decay laws.

In the following we make repeated use of Eq. 12. This expression contains explicitly, through $\langle\kappa^2\rangle$, the preaveraged angular distribution. This enables us to compare, for several geometries, Eq. 12 with the Förster-type expressions that follow from Eq. 7, where the orientational dependence is fully included into the decay law. In the same fashion as in Eqs. 9 to 11, we obtained from Eq. 7 the Förster-type form

$$\ln \Phi(t) \approx -p\rho \int d\mathbf{R}[1 - E(t_j\mathbf{R})]. \quad (13)$$

The remainder of this section is devoted to the evaluation of the decay laws $\Phi(t)$, for several orientational arrangements, with $w_a(\mathbf{R})$ being given by Eq. 1. We found it convenient to rewrite κ^2 in terms of the angles $\cos\psi \equiv \mathbf{e}_D \cdot \mathbf{e}_R$ and θ, where θ is the angle of $\mathbf{e}_A$ with the local field vector $\boldsymbol{\ell} \equiv \mathbf{e}_D - 3\,(\mathbf{e}_D \cdot \mathbf{e}_R)\,\mathbf{e}_R$. Then, as in reference 9

$$\kappa^2 = \ell^2 \mathbf{e}_A^2 \cos^2\vartheta = (1 + 3\cos^2\psi)\cos^2\vartheta. \quad (14)$$

The advantage of Eq. 14 is that it depends only on two angles.

Case a: Transition Dipoles of the Acceptors Randomly Distributed in Space

In this case all orientations of $\mathbf{e}_A$ in space are equally probable; the integration in Eq. 8 has to be performed in space, so that

$$E(t;\mathbf{R}) = (4\pi)^{-1} \int_0^{2\pi} d\varphi \int_0^\pi d\vartheta \sin\vartheta \exp[-f(t)\cos^2\vartheta]$$
$$= (\tfrac{1}{2}) \int_0^\pi d\vartheta \exp[-f(t)\cos^2\vartheta] \sin\vartheta \quad (15)$$

with

$$f(t) \equiv (1 + 3\cos^2\psi)\left(\frac{d}{R}\right)^6 \frac{t}{\tau}. \quad (16)$$

Setting $x = [f(t)]^{1/2}\cos\vartheta$ in Eq. 15 one obtains, using the integral representation of the error function, $\operatorname{erf} z = (2/\pi^{1/2}) \int_0^z \exp(-t^2)dt$, Eq. 7.1.1 of reference 16

$$E(t;\mathbf{R}) = (\tfrac{1}{2})\,[\pi/f(t)]^{1/2} \operatorname{erf}[\sqrt{f(t)}]. \quad (17)$$

Apart from the notational difference, this expression is identical to Eq. 2.21 of reference 9. To obtain the Förster-type decay, we have only to insert Eq. 17 into Eq. 13 and to perform the integration over the plane. We may now distinguish several special cases.

Case a1

The transition dipole of the donor is perpendicular to the plane of the molecules. Then $\cos\psi = \mathbf{e}_D \cdot \mathbf{e}_R = 0$ and $f(t) = (d/R)^6\,(t/\tau)$. From Eqs. 13 and 17 we obtain

$$\ln \Phi(t) = -p\rho 2\pi \int_0^\infty RdR$$
$$\cdot \{1 - \tfrac{1}{2}[\pi/f(t)]^{1/2} \operatorname{erf}[\sqrt{f(t)}]\} = -C_{a1}p\rho d^2(t/\tau)^{1/3} \quad (18)$$

with C_{a1} being a constant

$$C_{a1} = \frac{2\pi}{3} \int_0^\infty dx x^{-5/3}\{1 - [\sqrt{\pi}/(2x)] \operatorname{erf}(x)\}. \quad (19)$$

Integrating twice by parts we obtain

$$C_{a1} = \frac{2\pi}{3} \int_0^\infty dx\, x^{-8/3}\{x - (\sqrt{\pi}/2) \operatorname{erf}(x)\}$$
$$= \frac{2\pi}{5} \int_0^\infty dx\, x^{-5/3}[1 - \exp(-x^2)]$$
$$= \frac{6\pi}{5} \int_0^\infty dx\, x^{1/3} \exp(-x^2)$$
$$= \frac{3\pi}{5} \int_0^\infty dy\, y^{-1/3} \exp(-y) = \frac{3\pi}{5}\Gamma(\tfrac{2}{3}) = 2.55245. \quad (20)$$

This value may be compared with the preaveraged constant $\tilde{C}_{a1} = \pi\Gamma(\frac{2}{3})\,\langle\kappa^2\rangle^{1/3}$ of Eq. 12. Now, with Eq. 14, and remembering that $\cos^2\psi = 0$

$$\langle\kappa^2\rangle = \frac{1}{4\pi} \int_0^{2\pi} d\varphi \int_0^\pi d\vartheta \sin\vartheta \cos^2\vartheta = \int_0^1 x^2 dx = \tfrac{1}{3}. \quad (21)$$

Therefore $\tilde{C}_{a1} = 2.94962$ and the relative difference between C_{a1} and $\tilde{C}_{a1}$ is $C_{a1}/\tilde{C}_{a1} = 0.86535$.

Case a2

The transition dipole of the donor lies in the molecular plane. Inserting Eqs. 16 and 17 into Eq. 13 it follows

$$\ln \Phi(t) = p\rho \int_0^{2\pi} d\psi \int_0^R dR\, R$$
$$\cdot \{1 - \tfrac{1}{2}[\pi/f(t)]^{1/2} \operatorname{erf}[\sqrt{f(t)}]\} = -C_{a2}p\rho d^2(t/\tau)^{1/3} \quad (22)$$

with

$$C_{a2} = (C_{a1}/2\pi) \int_0^{2\pi} d\psi\, (1 + 3\cos^2\psi)^{1/3}, \qquad (23)$$

C_{a1} being given by Eq. 19. The integral of Eq. 23 is evaluated in the Appendix and equals 8.33625. Thus $C_{a2} = 3.38648$. In the case under study, the preaveraged $\langle \kappa^2 \rangle$ is given by

$$\langle \kappa^2 \rangle = \frac{1}{8\pi^2} \int_0^{2\pi} d\varphi \int_0^{\pi} d\vartheta \sin\vartheta \cdot \int_0^{2\pi} d\psi (1 + 3\cos^2\psi) \cos^2\vartheta = 2/5. \qquad (24)$$

Thus $\tilde{C}_{a2} = \pi\Gamma(2/3)\langle \kappa^2 \rangle^{1/3} = 4.00325$ and $C_{a2}/\tilde{C}_{a2} = 0.84593$.

Case a3

The directions of the transition dipoles of the donor and of the acceptors are randomly distributed in space. Under these circumstances, the preaveraged $\langle \kappa^2 \rangle$ equals

$$\langle \kappa^2 \rangle = (1/4) \int_0^{\pi} d\vartheta \sin\vartheta \int_0^{\pi} d\psi \sin\psi \cdot (1 + 3\cos^2\psi) \cos^2\vartheta = 2/3. \qquad (25)$$

Therefore $\tilde{C}_{a3} = \pi\Gamma(2/3)\langle \kappa^2 \rangle^{1/3} = 3.71629$.

In the same manner, C_{a3} follows through a slight change in Eq. 23

$$C_{a3} = (C_{a1}/2) \int_0^{\pi} d\psi (1 + 3\cos^2\psi)^{1/3} \sin\psi = C_{a1} \int_0^1 dx (1 + 3x^2)^{1/3} = C_{a1} \cdot 1.23288 = 3.14686. \qquad (26)$$

The quotient $C_{a3}/\tilde{C}_{a3}$ equals now $C_{a3}/\tilde{C}_{a3} = 0.84678$.

Case b: Transition Dipoles of Both Donor and Acceptors in the Plane; Acceptors Randomly Oriented

In this case all planar orientations of $\mathbf{e}_A$ are equally probable; thus from Eq. 8

$$E(t; \mathbf{R}) = \frac{1}{2\pi} \int_0^{2\pi} \exp[-f(t)\cos^2\vartheta] d\vartheta \qquad (27)$$

with $f(t)$ being given by Eq. 16. The integration of Eq. 27 leads to the modified Bessel function $I_0(z)$, Eqs. 9.6.1 of reference 16. Using the relation $\cos^2\vartheta = [1 + \cos(2\vartheta)]/2$ and the integral representation of $I_0(z) = (1/\pi) \int_0^{\pi} d\varphi \exp(-z\cos\varphi)$, Eq. 9.6.16 of reference 16, it follows

$$E(t; \mathbf{R}) = \exp[-f(t)/2]\, I_0[f(t)/2]. \qquad (28)$$

We have now only to insert Eq. 28 into Eq. 13 and to perform the integration over the plane. Through a variable substitution we obtain

$$\ln \Phi(t) = -p\rho \int_0^{\infty} dR\, R \int_0^{2\pi} d\psi [1 - E(t; \mathbf{R})] = -C_b p\rho\, d^2 (t/\tau)^{1/3} \qquad (29)$$

with

$$C_b = 2^{-1/3} (1/6) \int_0^{2\pi} d\psi (1 + 3\cos^2\psi)^{1/3} \cdot \int_0^{\infty} dx x^{-4/3} [1 - e^{-x} I_0(x)]. \qquad (30)$$

The constant C_b is evaluated in terms of higher transcendental functions in the appendix; its value is $C_b = 4.02525$.

We can now readily compare this constant with the preaveraged value $\tilde{C}_b = \pi\Gamma(2/3)\langle \kappa^2 \rangle^{1/3}$ of Eq. 12. Since all angular orientations in the plane are equally probable, one has from Eq. 14

$$\langle \kappa^2 \rangle = \frac{1}{(2\pi)^2} \int_0^{2\pi} \int_0^{2\pi} d\vartheta d\psi (1 + 3\cos^2\psi) \cos^2\vartheta = 5/4. \qquad (31)$$

Therefore $\tilde{C}_b = 4.58259$ and the relative difference between C_b and $\tilde{C}_b$ *is* $C_b/\tilde{C}_b = 0.87838$.

Case c: Transition Dipoles of Both Donor and Acceptors in the Plane; Acceptors Oriented Parallel to the Donor

Under these circumstances we have a perfect orientational order, and the disorder is limited to the positions of the acceptors. From Eq. 8 we obtain, by noting that $g(\alpha)$ is restricted to a single value

$$E(t; \mathbf{R}) = \exp[-(t/\tau)\,(d/R)^6 (1 - 3\cos^2\psi)^2], \qquad (32)$$

where we used Eqs. 1 and 2 directly. We insert now Eq. 32 into Eq. 13 and obtain for the Förster-type decay as in Eq. 12

$$\ln \Phi(t) = -p\rho \int_0^{2\pi} d\psi \int_0^{\infty} dR\, R[1 - E(t; \mathbf{R})] = -C_c p\rho\, d^2 (t/\tau)^{1/3} \qquad (33)$$

with

$$C_c = (1/2)\,\Gamma(2/3) \int_0^{2\pi} d\psi (1 - 3\cos^2\psi)^{2/3} = (1/2)\,\Gamma(2/3) \cdot 6.01925 = 4.07539. \qquad (34)$$

The preaveraged κ^2 factor corresponding to Eq. 32 is

$$\langle \kappa^2 \rangle = \frac{1}{2\pi} \int_0^{2\pi} (1 - 3\cos^2\psi)^2 d\psi = 1 - 6(1/3) + 9(3/8) = 19/8 \qquad (35)$$

by observing that $\langle \cos^2\psi \rangle = 1/3$ and $\langle \cos^4\psi \rangle = 3/8$. From Eq. 35 one has $\tilde{C}_c = \pi\Gamma(2/3)\langle \kappa^2 \rangle^{1/3} = 5.67580$. Therefore $C_c/\tilde{C}_c = 0.71803$.

Summarizing these results, we found that for all the orientational arrangements considered, the approximate Förster-type decays displayed the same time dependence as in Eq. 12. The geometrical restrictions imposed affected only the value of the constant C. Such a behavior was also noticed by Wolber and Hudson (1) for random orientations in space (our Case a3). In Table I we list the constants found, and give both the (static) C values, as well as the angularly preaveraged (dynamical) $\tilde{C}$ values.

TABLE I
CONSTANTS ENTERING THE FÖRSTER DECAY LAW, EQ. 12

Orientations*	C‡	$\tilde{C}$‡	$C/\tilde{C}$
Case a1	2.55245	2.94962	0.86535
Case a2	3.38648	4.00325	0.84593
Case a3	3.14686	3.71629	0.84678
Case b	4.02525	4.58259	0.87838
Case c	4.07539	5.67580	0.71803

*Orientations as in the text
‡C preaveraged, dynamic; $\tilde{C}$ static.

Apart from the case of a fixed orientation, where a significantly smaller value is found, in general the quotient $C/\tilde{C}$ is around 0.85. We note that in the three-dimensional case the corresponding quotient $C/\tilde{C}$ is 0.84518, as given by Blumen (9), Eq. 3.25; the value quoted corresponds to orientational disorder in space. This corroborates nicely with the observation of Dale et al. (2), who find numerically that the orientational preaveraging leads to an uncertainty of <20% in their R_0 values. In comparing our results with those in reference 9 we see that the orientational disorder leads to more interesting special cases for two- rather than for three-dimensional lattices. Nevertheless, the value $C/\tilde{C}$ is practically unchanged in going from three to two dimensions. This is atypical because disorder aspects tend in general to be enhanced if the dimension is lowered (8).

NUMERICAL RESULTS

In this section we evaluate numerically the exact decay laws and compare them with the previously discussed Förster-type expressions. We took as an underlying structure an infinite square lattice of lattice constant d. This choice has the advantage of simplicity and also allows a ready comparison with previous works (7, 8). We only note that the decay laws for more complex structures may be calculated along the same lines (7–9).

The numerical procedure amounts to computing the products, Eqs. 6 and 7, for different values of the concentration p and of the time, t, expressed in units of τ, i.e., t/τ. The time is varied from $(1/10)\,\tau$ to $10^5\tau$, whereas p varies between 0.002 and 1. Eqs. 6 and 7 are exact expressions and ensure a high accuracy of the results as no additional numerical averaging is necessary. To stress this point we performed straightforward evaluations not requiring any stochastic input such as random numbers; no Monte-Carlo procedure was involved.

Our results for different angular orientations are given in Figs. 1–4, in which both the exact decay (Eqs. 6 or 7) and also the appropriate Förster-type expression of the form $\exp(-Ct^{1/3})$ are presented. For the drawings, we choose to plot, as in former works (7–9), $-\ln(-\ln\Phi)$ vs. $\ln(t/\tau)$. Apart from the fact that this choice facilitates the comparison of the results, it has the advantage of representing the Förster-type forms as straight lines, so that decay laws corresponding to different concentrations are parallel shifted. As we will see in the following, in some cases the decay law for very short times and high concentrations is exponential; such an exponential behavior also appears as a straight line, but with a three times steeper slope; thus the short-time and the long-time decay regions are readily distinguished. Also our choice of scales allows us to show $\Phi(t)$ for a large range of time and concentration values and to emphasize the decay of the donor in the domain 90 to 1%, where the measurements are more precise than below 1%.

In Fig. 1 we present the decay for the dynamical case, in which donor and acceptors are randomly oriented in space and their rotational motion is rapid on the scale of the energy transfer. This results in the isotropic interactions of Eq. 3; this case was discussed by Wolber and Hudson (1) and also by Blumen and Manz (7). The exact decay law is

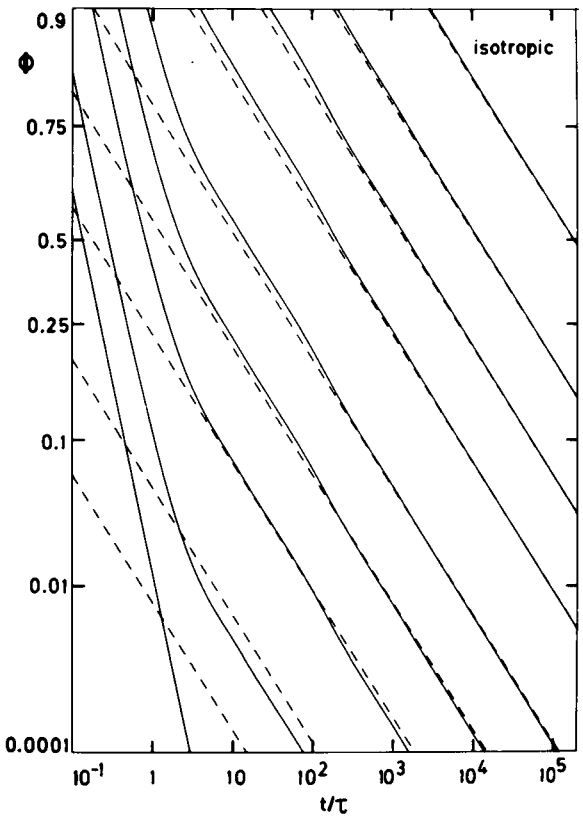

FIGURE 1 Time decay of the donor excitation $\Phi(t)$ due to the direct energy transfer via isotropic dipolar interactions. The acceptors occupy randomly sites on a square lattice. The curves depend parametrically on p; p is 1.0, 0.5, 0.2, 0.1, 0.05, 0.02, 0.01, 0.005, and 0.002 from the lower left corner to the upper right corner. The solid lines are the exact results, whereas the dashed curves are the Förster-type approximations. Note the $-\ln(-\ln\Phi)$ vs. $\ln(t/\tau)$ scales.

given by Eq. 6 and the approximate Förster-type expression by Eq. 12. Here, as in all other figures, the exact decay law is given as a full line, whereas the Förster-type decays are indicated by dashed lines. Evidently, the Förster-type expressions hold well for small values of p and for times longer than τ. As discussed in reference 7, the exact decay is quasi-exponential at short times; also, as may be readily verified from Eq. 6, for $p = 1$ the exact decay is exponential for all times. These facts are evident by inspection of Fig. 1. The waviness of the curves for intermediate values of p, $0.002 \leq p \leq 0.2$, and for times of the order 10τ are characteristic of the lattice structure. Comparison with other multipolar interactions (see reference 7) shows that here the waviness is less accentuated, a fact due to the smoothing, long-range behavior of the dipolar transfer. Thus, the presence of an underlying lattice is felt here through the short-time quasi-exponential decays, which stem from the existence of a minimal intermolecular distance d. From the drawing we infer that Förster-type decays are a good approximation of the true behavior for $p \leq 0.1$ and $t \geq 10\tau$.

Following our discussion of the previous section, we have also computed for different orientations of the donor the

decays due to acceptors randomly oriented in space (see our Cases a, a1–a3). The decay laws are very similar to Fig. 1 and differ from it mainly through their C values; since the C values are listed in Table I, we restrain from displaying the full decays.

Let us study the Cases b and c, in which the orientations of the transition dipoles are restricted to the molecular plane. In Fig. 2 we show the decay laws due to acceptors randomly oriented; the direction of the donor is parallel to the y-axis. The exact decay is the product over lattice sites, Eqs. 7 and 8

$$\Phi(t) = \prod_i [1 - p + pE(t; \mathbf{R}_i)], \tag{36}$$

where $E(t; \mathbf{R})$ is given by Eqs. 16 and 28. The Förster-type expression plotted is Eq. 29. Again, as in Fig. 1 there are deviations from the Förster approximation for high concentrations and at short times. Distinct from Fig. 1, the short-time high-concentration decay forms are nonexponential; this is due to the nonexponential form of $E(t; \mathbf{R})$, and has its physical roots in the orientational disorder. We have encountered a similar situation in reference 9 for the three-dimensional anisotropic decays. As in the previous case Eq. 29, the Förster-type form provides a good approximation of the decay law for longer times ($t \geq \tau$) and low to moderate ($p \leq 0.1$) acceptor concentrations.

We have also evaluated the decays for the case of the donor being oriented along a main diagonal of the square lattice. The curves are quite similar to the ones displayed in Fig. 2 and will not be given here.

Not to leave the reader under the impression that the orientation of the donor is always of little effect, we present in Figs. 3 and 4, counterexamples. Plotted are the decays for arrangements in which donor and acceptors are oriented parallel in the plane. In Fig. 3 all transition dipoles are along the y-axis, and in Fig. 4 they all point along a main diagonal. This is our Case c of the previous section. Here the Förster-type decays for both Figs. 3 and 4 are identical and are given by Eq. 33. The exact decay laws follow from the infinite product, Eq. 7, with $E(t; \mathbf{R})$ being given by Eq. 32. As is evident, the exact decays of Figs. 3 and 4 are considerably different; the difference lies in the short-time behavior and in the wavy pattern of the decay at moderate times. The short-time decay is here, as in Fig. 1, quasi-exponential, due to the lack of orientational disorder and exemplified by the exponential form of Eq. 32. Thus, the difference in the short-time decay rates of Figs. 3 and 4 is due to the differences in the values of $(1-3\cos^2\psi)^2$ for the two arrangements considered. As in the previous cases,

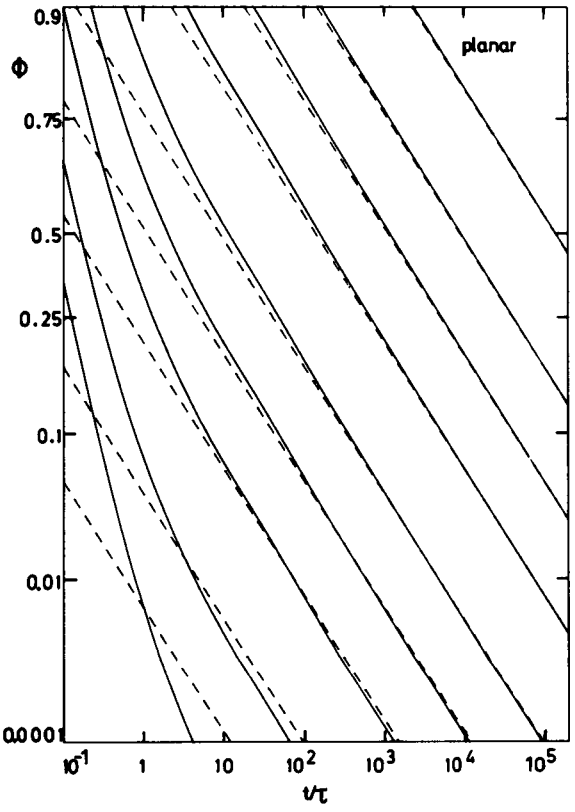

FIGURE 2 Time decay of the donor excitation $\Phi(t)$ due to anisotropic dipolar interactions. The acceptors occupy randomly sites on a square lattice, and their dipole moments are randomly oriented in the plane. The orientation of the donor dipole moment is along the y-axis. The values of the parameter p and the meaning of the solid and dashed curves are as in Fig. 1.

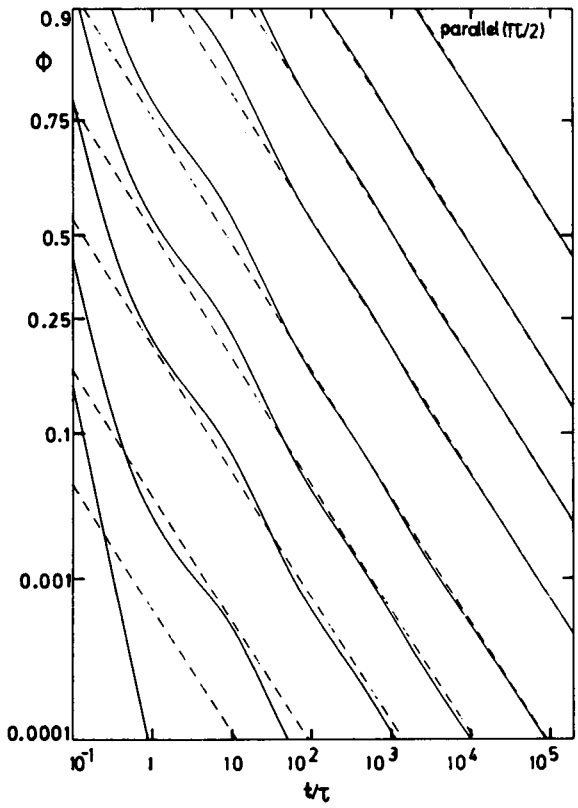

FIGURE 3 Time decay of the donor excitation $\Phi(t)$. The same situation as in Fig. 2 except that both donor and acceptors are oriented along the y-axis.

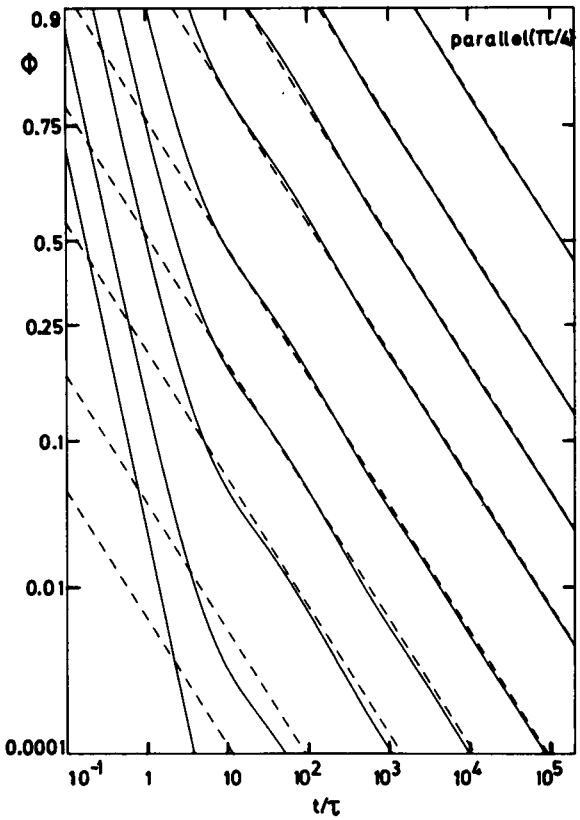

FIGURE 4 Time decay of the donor excitation $\Phi(t)$. The same situation as in Fig. 2 except that both donor and acceptors are oriented along a main diagonal of the square lattice.

we find that the agreement between the exact forms and the Förster-type decays is quite good for $t \geq 10\tau$ and $p \leq 0.1$.

CONCLUSIONS

Here we have studied the direct energy transfer to acceptors randomly distributed on the plane, and paid special attention to differences in the decay law, which are due to the anisotropy of the dipolar interaction; we also considered a series of different arrangements for the orientations of the transition dipole moments of donor and acceptors.

The major result to emerge is that the Förster-type formulas, Eq. 12 and the related expressions, provided a good description of the transfer laws for moderate and long times ($t \geq 10\tau$), and for acceptor concentrations up to 10% ($p = 0.1$). Only for fairly stiff geometrical constraints, as obtained when the orientations of the dipoles were restricted to one direction, did the lattice structure show up in the exact decay laws; this feature was absent from the Förster-type decays. At higher acceptor concentrations ($p > 0.2$), the quality of the Förster-type forms became rapidly poorer, partly because the major part of the decay shifted to lower times ($t \leq 10\tau$), which were not covered by these forms, and also because in this region the influence of the lattice structure grew. In this case we found it advisable to work directly with the exact decay law, Eq. 7, and not to revert to Monte-Carlo calculations (5); as discussed for the field of luminescence quenching in amorphous materials (17, 18), such time-consuming averaging calculations may be avoided by using the analytically averaged forms, Eq. 7. For all the models considered here, the Förster-type decays showed the same qualitative form. They were exponents of broken powers of the time (1, 7). The basic quantitative difference between the models (see Table I) was that the energy transfer became more effective if the geometric constraints forced the orientations to become more regular. The probability of the deexcitation of the donor grew by a factor of 2 in going from Case a1 to Case c. We conclude, as also pointed out in references 7 and 8, that a good knowledge of the microscopic rates allows one to use the measured luminescence decay to gain information on the underlying geometric order.

APPENDIX

Here we present the evaluation of integrals used in the main text. Consider first

$$J_1 \equiv \int_0^{2\pi} (1 + 3\cos^2\psi)^{1/3} d\psi, \tag{A1}$$

which appears in Eqs. 23 and 30. Inserting $\cos^2\psi = \frac{1}{2} \cdot (1 + \cos 2\psi)$ and making use of Eq. 3.664.1 of Gradshteyn and Ryzhik (19) one has

$$J_1 = 2^{2/3} \int_0^{\pi} (5 + 3\cos\varphi)^{1/3} d\varphi = 2^{4/3}\pi P_{1/3}(5/4), \tag{A2}$$

where $P_\nu(z)$ is the Legendre function. Eq. A2 gives J_1 in terms of a known analytical function. To evaluate it we start from the definition of $P_\nu(z)$ in terms of the hypergeometric function, Eq. 8.1.2 of reference 16, and use the corresponding series expansion, Eq. 15.1.1 of the same reference

$$\begin{aligned} J_1 &= 2^{4/3}\pi F(-1/3; 4/3; 1; -1/8) \\ &= 2^{4/3}\pi[\Gamma(-1/3)\Gamma(4/3)]^{-1} \sum_{n=0}^{\infty} \\ &\quad \Gamma(n - 1/3)\Gamma(n + 4/3)(n!)^{-2}(-1/8)^n. \end{aligned} \tag{A3}$$

Eq. A3 is an alternating, rapidly converging series. Using it we obtain $J_1 = 8.33625$.

The second integral to be considered is

$$J_2 \equiv \int_0^{\infty} dx\, x^{-4/3} [1 - e^{-x} I_0(x)], \tag{A4}$$

which appears in Eq. 30. Here, as in Eq. 30 $I_0(x)$ is the modified Bessel function of zero order, whose integral representation is $I_0(x) = 1/\pi \int_0^{\pi} \exp(-x\cos\varphi)\, d\varphi$. From this expression J_2 follows through an integration by parts

$$\begin{aligned} J_2 &= -3x^{-1/3}[1 - e^{-x} I_0(x)]\Big|_0^{\infty} \\ &\quad + (3/\pi) \int_0^{\infty} dx\, x^{-1/3} \int_0^{\pi} d\varphi (1 + \cos\varphi) \\ &\quad \cdot \exp[-x(1 + \cos\varphi)]. \end{aligned} \tag{A5}$$

The first term on the right side of Eq. A5 vanishes, and the substitution

$y = x(1 + \cos\varphi)$ leads to

$$J_2 = (3/\pi)\,\Gamma(2/3)\int_0^{\pi}(1 + \cos\varphi)^{1/3}\,d\varphi. \qquad \text{(A6)}$$

The angular integration proceeds as follows

$$\begin{aligned}\int_0^{\pi}(1 + \cos\varphi)^{1/3}d\varphi &= \int_0^{\pi}(1 + \cos 2\theta)^{1/3}d\theta \\ &= 2^{4/3}\int_0^{\pi/2}\cos^{2/3}\theta d\theta \\ &= 2^{4/3}2^{-1/3}[\Gamma(5/6)]^2/\Gamma(5/3) \qquad \text{(A7)}\end{aligned}$$

where in the last line Eqs. 3.621.1 and 8.384 of reference 19 were inserted. Collecting terms we find for J_2

$$J_2 = (9/\pi)[\Gamma(5/6)]^2 = 3.65020. \qquad \text{(A8)}$$

From J_1 and J_2 one obtains for C_b in Eq. 30 $C_b = 4.02525$.

The authors are very thankful to Professor G. L. Hofacker for his support. The computations were performed on the CYBER 175 computer of the Bayerische Akademie der Wissenschaften.

Grants from the Deutsche Forschungsgemeinschaft and the Fonds der Chemischen Industrie are gratefully acknowledged.

Received for publication 8 August 1983.

Note Added in Proof: We recently became aware of reference 20, which obtained the results for the two- (our Case a3) and one-dimensional problems in the continuum limit (9, 20).

REFERENCES

1. Wolber, P. K., and B. S. Hudson. 1979. An analytical solution to the Förster energy transfer problem in two dimensions. *Biophys. J.* 28:197–201.
2. Dale, R. E., J. Eisinger, and W. E. Blumberg. 1979. The orientational freedom of molecular probes. The orientation factor in intramolecular energy transfer. *Biophys. J.* 26:161–194.
3. Estep, T. N., and T. E. Thompson. 1979. Energy transfer in lipid bilayers. *Biophys. J.* 26:195–208.
4. Dewey, T. G., and G. G. Hammes. 1980. Calculation of fluorescence resonance energy transfer on surfaces. *Biophys. J.* 32:1023–1036.
5. Snyder, B., and E. Freire. 1982. Fluorescence energy transfer in two dimensions. A numeric solution for random and nonrandom distributions. *Biophys. J.* 40:137–148.
6. Förster, T. 1949. Experimentelle und theoretische Untersuchung des zwischenmolekularen Übergangs von Elektronenanregungsenergie. *Z. Naturforsch. A.* 4:321–327.
7. Blumen, A., and J. Manz. 1979. On the concentration and time dependence of the energy transfer to randomly distributed acceptors. *J. Chem. Phys.* 71:4694–4702.
8. Blumen, A. 1981. Excitation transfer from a donor to acceptors in condensed media. A unified approach. *Nuovo Cimento B.* 63:50–58.
9. Blumen, A. 1981. On the anisotropic energy transfer to random acceptors. *J. Chem. Phys.* 74:6926–6933.
10. Stryer, L. 1978. Fluorescence energy transfer as a spectroscopic ruler. *Ann. Rev. Biochem.* 47:819–846.
11. Knox, R. S. 1975. Excitation energy transfer and migration: theoretical considerations. *In* Bioenergetics of Photosynthesis. Govindjee, editor (Academic Press, Inc., New York). 183–221.
12. Galanin, M. D. 1955. The problem of the effect of concentration on the luminescence of solutions. *Zh. Eksp. Teor. Fiz.* 28:485–495.
13. Förster, T. 1965. Delocalized excitation and excitation transfer. *In* Modern Quantum Chemistry. O. Sinanoğlu, Academic Press, Inc., New York. 3:93–137.
14. Knox, R. S. 1977. Photosynthetic efficiency and exciton transfer and trapping. *In* Topics in Photosynthesis. J. Barber, editor. Elsevier/North Holland, Amsterdam. 2:55–97.
15. Swenberg, C. E. 1982. Fluorescence decay kinetics and bimolecular processes in photosynthetic membranes. *In* Biological Events Probed by Ultrafast Laser Spectroscopy. R. R. Alfano, editor. Academic Press, Inc., New York. 193.
16. Abramowitz, M., and I. A. Stegun. 1972. Handbook of mathematical functions. Dover Publications, Inc., New York.
17. Blumen, A., and J. Klafter. 1983. Quenching of luminescence by non-radiative tunnelling. *Phil. Mag. B.* 47:L5–8.
18. Searle, T. M. 1983. Photoluminescence efficiencies and yields in disordered systems. *Solid State Commun.* 46:291–293.
19. Gradshteyn, I. S., and I. M. Ryzhik. 1965. Table of Integrals, Series and Products. Fourth ed. Academic Press, Inc., New York.
20. Fredrickson, G. H., and C. W. Frank. 1983. Interpretation of electronic-energy transport in polymeric systems. *Macromolecules.* 6:1198–1206.